Chapter 2

SEA-SALT AEROSOLS

"I must go down to the sea again, for the call of the running tide
Is a wild call and a clear call that may not be denied;
And all I ask is a windy day with the white clouds flying,
And the flung spray and the blown spume, and the sea-gulls crying."

John Masefield, *SEA-FEVER*

Aerosols are stable microscopic particles or droplets suspended in the atmosphere. The open ocean is one of the major sources of natural aerosols, producing annually 10^{15}-10^{16} g of sea-salt aerosols. Sea-salt aerosols, together with wind-blown mineral dust, and naturally occurring sulfates and organic compounds, are part of natural tropospheric aerosols. In remote air, these aerosols set the baseline concentration of a background atmosphere, one that exists in the absence of anthropogenic perturbation (Whittlestone et al., 1998). On a planet covered with more than 70% ocean surface and landmasses clustered mostly in one hemisphere, remote pristine air with baseline concentrations of atmospheric constituents represents a large portion of the surface-atmosphere system. Physical and chemical properties of the background aerosols affect the radiative processes in clean atmosphere, namely reflection, transmission, and absorption. The following review of the formation, properties, significance, and modeling of sea-salt aerosols and whitecaps gives a basis for the formulation of the scientific objectives of the current research.

2.1 Formation of sea-salt aerosols

Historically, meteorologists initiated the search for the origin of sea salts in the atmosphere. They were looking for sources of condensation nuclei since the experiments of John Aitken and C.T.R. Wilson had shown that without such nuclei, water vapor would not condense into cloud droplets, rain, fog, or snow at ordinary air humidity (Jacobs, 1937). In 1881, Aitken suggested the ocean as the primary source of condensation nuclei (Blanchard, 1963). By analogy to laboratory observations of collapsing bubbles, Jacobs (1937) first assumed that in the ocean the breaking of waves and bursting of bubbles produce sea-salt aerosols. Boyce (1951) found experimentally that most of these particles are produced within foamy whitecaps formed when waves break. Fast-speed photography documented the exact mechanism of bubble bursting and drop formation (Woodcock et al., 1953; Kientzler et al., 1954).

Sea-salt aerosols form by evaporation of sea-spray droplets produced by bubble bursting within foamy whitecaps and wind tearing off the wave crests. Current knowledge on sea spray encompasses three types of spray droplets, named after their production mechanisms: film, jet, and spume drops (Blanchard, 1983; Wu, 1992a; Andreas et al., 1995). As wind blows over the ocean, waves break and entrain air into the water forming clouds of bubbles beneath and foam patches on the surface. Once formed, the bubbles start rising to the surface due to their buoyancy. The bubbles reaching the open surface are responsible for the formation of sea spray. While they float on the surface, the film caps, separating the air inside the bubbles from the air outside, thin and the bubbles burst producing drops by two mechanisms (Blanchard, 1963; MacIntyre, 1972; Resch and Afeti, 1991; Spiel, 1995). In the first mechanism, the shattering of the film caps generates 10s to 100s of small droplets called film drops. Film drops span a size range from a physically possible minimum of 0.1 μm radius to a

typical value of 50 μm with a peak about 1-2.5 μm (Andreas, 2002). In the second mechanism, a water jet projects with high acceleration upward from the collapsing bubble cavity, becomes unstable, and breaks up into several droplets called jet drops. Depending on the bubble size, 1 to 10 jet drops are ejected into the air from the tip of the jet. Jet drop radii range from 1 to 300 μm, with a peak around 10 μm (Andreas, 2002). These two ways of producing droplets are indirect, i.e., mediated by the bubbles within the whitecaps. A third, direct, mechanism for spray generation is via mechanical disruption of wave crests under strong winds. At high wind speeds, above 9 m s^{-1}, spume drops are torn from the wave crests and blown directly into the air. Spume drops are relatively large, with radii starting from 20 μm and reaching more than 500 μm (Andreas, 2002). Altogether, sea spray droplets cover a size range of 0.1-500 μm radii as shown in the upper part of Figure 2.1.

Driven out of the sea and entering the atmosphere, sea spray droplets get into an environment different from their watery milieu. Normally, the air is drier, with relative humidity (RH) less than 100%, and film, jet, and spume droplets start to evaporate. They eventually equilibrate with the ambient RH, and, becoming smaller, stable and long-lived, develop into sea-salt aerosols (Blanchard, 1983). Not all sea spray droplets transform into sea-salt aerosols. Many drops return to the sea almost immediately; the largest, > 100 μm, stay less than 0.5 s in the air (Andreas, 1992). Under winds of 5 m s^{-1}, 20-100 μm drops linger for at most 10 s, and settle down before reaching moisture equilibrium. Sea spray with radii < 20 μm reside in the air for more than 10 s, and succeed in reaching moisture equilibrium. With that the process of formation of sea-salt aerosols ends. These so formed sea-salt aerosols are the subject of investigation in this study.

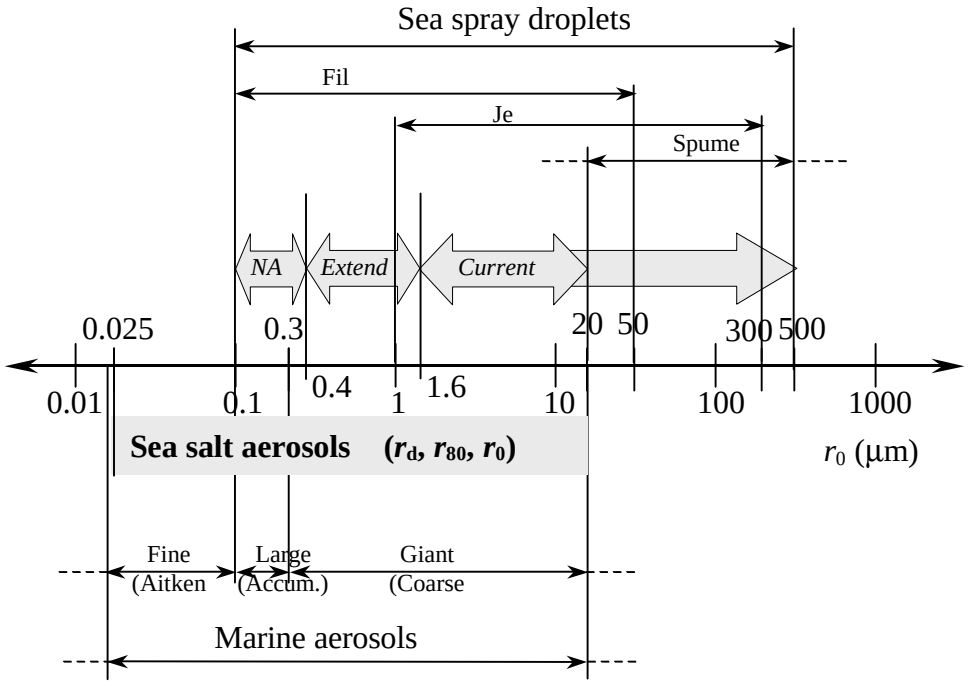

Figure 2.1 Schematic comparisons of the sizes of sea spray droplets (r_0, μm) (Andreas, 2002), the sizes of marine aerosols (r_0, r_{80}, or r_d μm) (Bates et al., 1998b), and the sizes modeled by the sea-salt aerosol function (*Current* (Andreas, 2002), *Extend* (Monahan et al., 1986), *NA* (Not Available); details in the text).

2.2 Properties of sea-salt aerosols

Chemical and physical processes occurring under various environmental conditions constantly rework sea-salt aerosols during their lifetime, about 2 days (Keene et al., 1998). Participating in chemical reactions and losing water mass by evaporation, sea-salt aerosols attain altered chemical composition, higher salt concentrations, different phase states, and various sizes. The physicochemical properties of sea-salt aerosols determine their optical properties; any changes in the

former invoke changes in the later. Thus, the chemical, physical and optical properties of aged sea-salt aerosols are quite different from those of fresh sea-salt aerosols.

2.2.1 Chemical properties

Chemical composition

At the moment of their production, film, jet, and spume drops have chemical composition and pH close to that of normal seawater; the fresh sea-salt aerosols inherit these. The ratios of the major seawater ions are preserved in the newly formed aerosols (Table 7-15 in Warneck, 1988). Sea-salt aerosols are alkaline with pH about 7.0 to 8.7 (Keene et al., 1998). A specific feature of the fresh sea-salt aerosols, transferred to aged sea-salt aerosols, is their enrichment with organic matter (Blanchard, 1963; Middlebrook et al., 1998), iodine (Cicerone, 1981;Warneck, 1988; Murphy et al., 1997), and even live organisms, bacteria (Blanchard and Syzdek, 1970; Blanchard, 1983) or neuston (Zaitsev, 1997).

Sodium chloride (NaCl) is 85% of all salts comprising the salt content of seawater, and well represents the initial chemical composition of sea spray and fresh sea-salt aerosols (Blanchard, 1983; Chameides and Stelson, 1992; Sellegri et al., 2001; Moldanová and Ljungström, 2001). Sulfates ($CaSO_4$, $MgSO_4$) and chlorides ($MgCl_2$, KCl) mix with NaCl and make sea-salt aerosols highly hygroscopic multicomponent aerosols (Cheng, 1993; Tang and Munkelwitz, 1994; Tang et al., 1997). Sea-salt aerosols readily absorb moisture from the atmosphere since their various components have a wide range of deliquescent points, from 33% for $MgCl_2$ to 75% for NaCl to 88% for $MgSO_4$ (Table 7-6 in Warneck, 1988). Thus, at typical RH, sea-salt aerosols are deliquescent particles containing highly concentrated solution of water-soluble salts.

The most important consequence of having such a chemical composition is that under certain condition sea-salt aerosols can act as cloud condensation nuclei (CCN) more effectively than other aerosol species.

Chemical transformation

As deliquescent drops or dry particles, sea-salt aerosols are unique media in which chemical reactions take place. Chemical reactions proceeding in the bulk of deliquescent or on the surface of dry particles are referred to as multiphase and heterogeneous chemistry, respectively (Ravishankara, 1997). Because of multiphase and heterogeneous reactions, aged sea-salt aerosols are acidic, dechlorinated, and sulfate enriched compared to fresh sea-salt aerosols.

Alkaline sea-salt aerosols rapidly become acidic, within about 15 min (Keene et al., 1998). The process starts with direct scavenging of acids from the atmosphere by sea-salt aerosols, e.g., sulfuric acid (H_2SO_4), nitric acid (HNO_3), and hydrochloric acid (HCl). The acids dissolve in the drops, then dissociate, releasing hydrogen ions (H^+). Initially, H^+ titrate the sea-salt alkalinity, that is, they neutralize the negative ions within the sea-salt aerosols such as bicarbonate (HCO_3^-), carbonate (CO_3^{2-}), borate ($H_2BO_3^-$), and hydroxyl (OH^-). When all negative ions are neutralized, H^+ starts to gradually accumulate acidifying the sea-salt droplets (Keene et al., 1998; Erickson et al., 1999).

Dechlorination is a process of replacement of chlorine ions (Cl^-) in sea-salt aerosols by other ions. The process starts when the sea-salt aerosols become acidic with pH below 7, which allows multiphase reactions to proceed and displace Cl^- (Keene et al., 1998). There are four types of reactions dechlorinating the sea-salt aerosols

(Keene et al., 1990; Graedel and Keene, 1995; Mozurkewich, 1995; Erickson et al., 1999; Sellegri et al., 2001). One is acid displacement, in which

$$H_2SO_4(g) + 2NaCl(p) \rightarrow 2HCl(g) + Na_2SO_4(p)$$

$$HNO_3(g) + NaCl(p) \rightarrow HCl(g) + NaNO_3(p) \qquad (R1)$$

where NaCl(p) represents sea-salt aerosol. As pH further decreases to < 4, HCl volatilizes from the particle, transporting Cl^- into the air. Another process for losing Cl^- involves reactions with nonacidic dinitrogen pentoxide (N_2O_5) during the night, in which N_2O_5 is involved in the process instead of acids. Alternatively, reactions of Cl^- with free radicals in sea-salt aerosols also yield losses of Cl^-. Finally, heterogeneous reactions with metals on dust particles enhances Cl^- deficit in the presence of windblown continental dust.

Similar reactions also drive bromide (Br) out of the sea-salt aerosols. Bromic acid (HBr), scavenged from the atmosphere, volatilizes from the sea-salt aerosols at pH < 2 in form of HBr or molecular bromide (Br_2), and depletes them of Br^- (Mozurkewich, 1995; Sander and Crutzen, 1996).

While multiphase reactions in sea-salt aerosols expel the halogen ions, Cl^- and Br^-, Na sulfates and nitrates accumulate as reactions (R1) above suggest (Murphy et al., 1998a). These gradually change the chemical composition of fresh sea-salt aerosols from a mixture of sulfates and chlorides to a mixture of sulfates and nitrates. Aged sea-salt particles are still quite soluble and potentially important as CCN, since both SO_4^{2-} and NO_3^- ions form soluble species with Ca^{2+} and Mg^{2+} within the aerosols (Table 7-6 in Warneck, 1988; Murphy et al., 1998a). Meanwhile, the amount of Na remains the same, especially in clean marine air not containing crustal dust or anthropogenic aerosols, and its presence is a good tracer for particles originating from

sea-salt aerosols (Duce et al., 1983; Keene et al., 1986, Murphy et al., 1998a). Using the constancy of Na in reworked sea-salt aerosols, the dehalogenation and sulfate enrichment can be detected from changes in the seawater ratios (Table 7-15 in Warneck, 1988). In any type of aerosols, the SO_4^{2-}, which is in excess of the SO_4^{2-} normally found in sweater, is referred to as non-sea-salt sulfate (nss SO_4^{2-}). Large particles, 1-6 μm, with excess SO_4^{2-} have been detected, and the only mechanism completely explaining such observations is multiphase reactions within sea-salt aerosols (Luria and Sievering, 1991; Sievering et al., 1992).

These chemical transformations of sea-salt aerosols are more pronounced in coastal zones than in remote regions of the ocean. Abundant acids in continental, usually polluted, air masses initiate and sustain the process of acidification yielding to significant dehalogenation and respective SO_4^{2-} enrichment, especially in submicron (< 1μm) sea-salt aerosols (Clegg and Toumi, 1998; Erickson et al., 1999; Quinn et al., 2000). In clean remote air, where the concentrations of acids are not enough to titrate the sea-salt alkalinity completely, the dehalogenation of sea-salt aerosols is not significant (Murphy et al., 1998a).

This concise description oversimplifies the multiphase chemical processes occurring in deliquescent sea-salt aerosols. Several models give a full account of the possible reactions and reagents involved in the halogen chemistry within sea-salt aerosols (Chameides and Stelson, 1992; Sander and Crutzen, 1996; Moldanová and Ljungström, 2001).

2.2.2 Physical properties

Phase state

Sea-salt aerosols, left behind by sea-spray droplets after evaporation, exist in the air as liquid drops, deliquescent drops, or dry sea-salt particles depending on the RH (Blanchard, 1983; Warneck, 1988; Tang et al., 1997; Keene et al., 1998). If RH is high, ≈ 100%, film, jet, and spume droplets remain liquid, and retain the sizes of the parent spray droplets. At lower RH, but above 75%, the deliquescence point of NaCl (§2.2.1), sea-salt aerosols reside in the air as deliquescent particles. Their radii are about half of the radii of the parent droplets at 80% RH (Fitzgerald, 1975; Monahan, 1986). At RH < 75%, the drops crystallize into a kind of dry sea-salt particles, and their diameters shrink to about one quarter that of the parent drops (Blanchard, 1983). Even at very low RH about 50-60%, sea-salt aerosols are never completely dry, because of the low deliquescence of $MgCl_2$. Of all possible phase states, deliquescent drops are the usual state of sea-salt aerosols since atmospheric RH typically ranges from 75% to 100% (Warneck, 1988). In all states of existence, sea-salt aerosols are spherical, or at least roundish (Cheng et al., 1988; Mitra et al., 1992). This is an important fact for models assuming and considering the sea-salt aerosols as spheres.

Size

The size of sea-salt aerosols is defined by radius or diameter, assuming they are spherical. With initial sea spray radii spanning 0.1-20 μm range and phase transformations in the atmosphere, one may expect sea-salt aerosols in the range 0.025 μm to 20 μm radii to exist, Figure 2.1. Field experiments at different locations, from clean remote areas to coastal zones, using different measuring techniques have documented sea-salt aerosols with radii in the range 0.05-6 μm (Mészarós and Vissy,

1974; O'Dowd and Smith, 1993; Kreidenweis et al., 1998; Murphy et al., 1998b; Quinn and Coffman, 1999; Reid et al., 2001). With such sizes, sea-salt aerosols are present in the accumulation and coarse modes, sometimes in the nucleation mode, of a typical marine aerosol size spectrum, which spans from 0.0025 μm to 20 μm (Warneck, 1988; Fitzgerald, 1991; Andreae, 1995; Bates et al., 1998b), Figure 2.1.

Size distribution

A size distribution refers to number density of the particles as a function of the particle size, dN/dr. Often the form $dN/d(\log r)$ is used to accommodate the orders of magnitude variations of particle radii and number densities. Size distribution of any other property of the aerosols that varies with particle size, e.g., particle surface, volume, or mass, can be derived from that of number density by applying the appropriate weights (Warneck, 1988, p. 283). A typical feature of the size distribution of sea-salt aerosols is a decrease in the number of particles with increasing radius since gravitational settling increases with size (Fitzgerald, 1991; Smith et al., 1993; O'Dowd et al., 1997; Reid et al., 2001). While fewer in number, however, particles in the large end of the size distribution contribute most to the particle surface, volume, or mass available in the atmosphere.

Concentration

The number and mass concentration of sea-salt aerosols are defined as the total number of particles and the total mass of sea salt for all sizes per unit volume in units [m^{-3}] and [$\mu g\ m^{-3}$] respectively. Both can be measured independently or derived from measured or modeled number size distribution, *dN*/*dr*, by integration over all sizes. The surface [$m^2\ m^{-3}$] and volume [$m^3\ m^{-3}$] concentration can also be computed

from the number size distribution. Kreidenweis et al. (1998) report that in clean air masses, sea-salt number concentration ranges from about 50 to 100 cm^{-3}. In terms of mass concentration, sea salts at different locations range from 1.2 to 55 $\mu g\ m^{-3}$ (Fitzgerald, 1991; Quinn et al., 2000).

Flux

Balancing the fluxes of produced and deposited sea-salt aerosols, Eriksson (1959) first estimated that oceans deliver 10^{15} g of sea salts annually. Blanchard (1963, 1985) obtained a value of 10^{16} g yr^{-1} after refining Eriksson's parameterization of the deposition flux. Numerous other estimations, all of them falling in the range between these two extrema, were offered (Erickson and Duce, 1988; Andreae, 1995; Gong et al., 1997b; Tegen et al., 1997). Causes for the discrepancies are: use of different parameterizations of production and deposition fluxes; mean, instead of instantaneous, values of wind speed; and integration of sea-salt cycling over atmospheric layers with different thicknesses.

Variability

Size distribution and concentration of sea-salt aerosols vary substantially in time and space. Size distribution shows an increase of number density of sea-salt aerosols with wind, especially at the large-size end (Monahan et al., 1983a; Smith et al., 1993; O'Dowd et al., 1997, Reid et al., 2001). Sea-salt concentration rises from about 2 to 50 $\mu g\ m^{-3}$ for winds less than 10 m s^{-1}, and reaches up to 161 $\mu g\ m^{-3}$ at winds greater than 10 m s^{-1} (Fitzgerald, 1991; Kreidenweis et al., 1998). Sea-salt number and mass concentration exhibit a rapid decrease of 2-3 orders of magnitude in the first 2 km above the ocean (Woodcock; 1953; Reid et al.; 2001). Sea-salt concentration usually

decreases with distance away from the shoreline (Woodcock, 1953), though for submicron particles Reid et al. (2001) measured an increase at 40 km from the coast as the wind increased to 12 m s^{-1}. Globally, sea-salt concentration varies from 10-15 μg m^{-3} in the equatorial regions to 40-49 μg m^{-3} in the higher latitudes (Erickson et al., 1986; Fitzgerald, 1991). Sea-salt mass concentration exhibits substantial seasonal dependence, with differences in winter and summer estimates of a factor of 2-3, mainly due to the seasonal variations of the wind speed (Erickson et al., 1986). Despite this variability, sea-salt aerosol concentration is relatively constant in time and space compared to other aerosol types (e.g., mineral dust) because the entire ocean surface is a source of sea-salt aerosols all the time (Tegen et al., 1997; Tegen, 1999).

Relative presence

Total aerosol loading comprises different aerosol species, and each of these species exhibits its own physical and chemical properties. Since these properties vary with environmental conditions, natural and anthropogenic factors, as well as aerosol source placement, establish one or another aerosol species as a dominant species of the total aerosol loading. The characteristics of the dominant species determine the overall effects of the total aerosol loading. The first Aerosol Characterization Experiment (ACE-1) indicates that in terms of number and mass concentration, sea-salt aerosols are the dominant species of the accumulation and coarse modes in remote air minimally perturbed by continental and anthropogenic aerosol sources (Bates et al., 1998a, 1998b; Murphy et al, 1998b; Quinn et al., 1998; Kreidenweis et al., 1998; Quinn and Coffman, 1999). Sea-salt aerosols, therefore, determine overall characteristics of the background marine aerosols. ACE-2 showed that in polluted air the role of sea-salt aerosols in defining the properties of the total aerosol load was relatively small, despite

the fact that sea-salt aerosol concentration in accumulation and coarse modes were comparable to those measured during ACE-1 (Quinn et al., 2000). The reason was the order of magnitude difference in the concentrations of the sulfates aerosols, especially the submicron ones, measured in clean and polluted air. Submicron nss SO_4^{2-} aerosols control the properties of the total aerosol loading in marine air masses impacted by continental aerosols.

2.2.3 Optical properties

The solar radiation attenuates as it propagates through the atmosphere due to Rayleigh scattering and absorption by air molecules, and Mie scattering and absorption by atmospheric aerosols. Sea-salt aerosols, assumed to be nonabsorbent particles (Winter and Chýlek, 1997; Quinn et al, 1996; 1998), attenuate the solar flux reaching Earth's surface and add to the flux reflected back to space mostly by scattering. Basic parameters quantifying changes in the solar radiation due to sea-salt aerosols are scattering/backscattering coefficients, k_s and k_{bs}, and optical thickness, t.

Particles in accumulation and coarse modes with diameters from 0.08 to 3 μm scatter visible light most efficiently (Andreae, 1995; Quinn et al., 1996; Murphy et al., 1998b). Field experiments reveal that in the submicron range, the scattering coefficient of sea-salt aerosols is comparable to that of nss SO_4^{2-} particles (Figure 2 in Quinn and Coffman, 1999). Analytical considerations show that the scattering coefficient decreases at supermicron sizes, > 1 μm, but because of their abundance, sea-salt aerosols compensate the low efficiency, and largely control the light scattering at these sizes (Quinn et al., 1996; Carrico et al., 1998). Overall, sea-salt aerosols control the radiative effects in a background atmosphere due to their dominance in both sub- and supermicron sizes. Murphy et al. (1998b) find that in the Southern Ocean,

sea-salt particles are responsible for about 95% of the aerosol light scattering, with over 75% provided by the submicron sea salts alone. In polluted air, the contribution of sea-salt aerosols is comparable to that of the SO_4^{2-} aerosols. Averaged over different locations, the scattering due to sub- and supermicron sea-salt aerosols ranges from 97% down to 63%, of this 42% to 23% are due to submicron sized sea-salt particles alone (Quinn and Coffman, 1999). The efficiency of sea-salt light scattering decreases as sea-salt aerosols lose Cl^- (Tang et al., 1997).

2.3 Climate system and sea-salt aerosols

As an intrinsic part of the atmospheric marine boundary layer (MBL), sea-salt aerosols play an active role in the climate system. They contribute to variations of the radiative field of the atmosphere directly by reflecting solar radiation back to space, and indirectly by acting as CCN (Andreae, 1995). In addition, halogen chemistry in and on sea-salt aerosols affects the concentration and distribution of atmospheric constituents (Andreae and Crutzen, 1997).

2.3.1 Relative significance

Aerosol sizes from about 0.08 to 1 μm diameter are the most efficient for both scattering of shortwave radiation and acting as CCN, the respective bases for direct and indirect forcing. In the MBL, often the most numerous submicron aerosols are nss SO_4^{2-} particles around and below 0.08 μm (Hoppel et al., 1996), while most aerosols around and above 1 μm diameter are sea-salts. Thus, the relative importance of sea-salt and nss SO_4^{2-} aerosols for the climate processes has been a subject of an on-going debate.

In 1987, Charlson and colleagues put forward the hypothesis that a feedback loop involving marine phytoplankton, sulfate aerosol formation, and cloud albedo might stabilize the Earth's temperature (Charlson et al., 1987). Since then, vigorous investigations of the climatic effects of sulfate aerosols usually overshadow the involvement of sea-salt aerosols in the direct and indirect forcing because of two assumptions. First, sea-salt particles are too large to participate effectively in scattering solar radiation and acting as CCN. Second, the effective submicron particles are overwhelmingly nss SO_4^{2-} rather than sea-salt aerosols (Hobbs, 1971; Charlson et al., 1987; Andreae, 1995). These assumptions are well justified for continental, polluted, and modified marine air masses (Hoppel et al., 1996; Quinn et al., 2000). It becomes clear, then, how easy it is to underestimate the role of sea-salt aerosols.

Recent measurements in remote regions (Bates et al., 1998b) have proven, however, that these assumptions are not always valid, and lead to underestimation of sea-salt aerosol effects. For both sub- and supermicron sizes, sea-salt aerosols are the dominant constituent of the total aerosol loading in vast regions with clean marine air (§2.2.2), hence the quantification of baseline atmospheric processes must reckon with their presence. Further, in polluted and continental air, sea-salt aerosols either enhance or diminish the effects of the anthropogenic sulfates.

2.3.2 Direct forcing

The most prominent role of sea-salt aerosols is in the direct increase of the planetary albedo through scattering of solar radiation. Sea-salt aerosols are the leading contributor to direct radiative forcing in the background atmosphere.

Tegen et al. (1997) modeled the direct effects of different aerosols species, and found a maximum contribution of sea-salt aerosols to the total aerosol extinction of

21-27% in high latitudes, and 10-15% in low latitudes. These are surprisingly low values and are far from the results of other analytical and experimental studies (§2.2.3). The reason is that Tegen et al. (1997) assumed a minimum diameter of sea-salt particles of 4 μm (!), a sad illustration of the misconception about sea-salt aerosols. Corrected assumptions reconcile their model results with the others (Tegen, 1999).

Haywood et al. (1999) modeled the solar irradiance at the top of the atmosphere without and with different natural and anthropogenic aerosols and compared the computed values with those observed by the Earth Radiation Budget Experiment (ERBE). Without aerosols, the model underestimated the solar irradiance over the entire globe, indicating that an important reflective component was missing in the surface-atmosphere system. The bias was compensated to some degree when all aerosol types, except sea salts, were considered, especially in the Northern hemisphere, where modeled and observed values balanced each other. Only the inclusion of sea-salt aerosols, however, brought about the best balance between model and measurements.

The direct forcing of sea-salt aerosols is estimated as ≅ 0.6 to 2 W m^{-2} cooling of the current climate for an environment of 70 to 99% RH (Winter and Chýlek, 1997; Jacobson, 2001a). In a warmer world with increased wind speeds leading to enhanced production of sea spray, the cooling potential of sea-salt aerosols can double and reach -4 W m^{-2}.

2.3.3 Indirect forcing

Sea-salt aerosols either dominate the activation of CCN or influence the activation on sulfate aerosols, depending on the surrounding conditions.

The concentration of CCN available in the atmosphere controls the number of cloud droplets hence cloud albedo and lifetime. CCN are submicron atmospheric

particles, whose presence initiate cloud drop growth at supersaturation that is much lower, 2×10^{-4}% to 0.5%, than the supersaturation required for nucleation of homogenous water vapor, about 300% (Andreae, 1995). At certain critical supersaturation levels, water condensation begins on the largest and most soluble aerosol particles (Andreae, 1995; Murphy et al., 1998b). In a mixture of particles with different sizes and solubility the principle is: the larger and the more soluble the particle, the lower the supersaturation threshold. Particles, which meet these requirements at given supersaturation, are activated and grow rapidly into cloud droplets. Any soluble aerosols with sizes above 0.05 μm in diameter can serve as CCN at supersaturations below 0.5%.

Typical supersaturations in marine clouds are of the order of 0.2-0.3% (O'Dowd et al., 1997). Such supersaturations activate particles in accumulation and coarse modes with sizes above 0.08 μm diameter (Andreae, 1995). Both sea-salt and nss SO_4^{2-} aerosols are eligible to act as CCN because of their high solubility and presence in this size range. Being larger than, or comparable to, nss SO_4^{2-} aerosol sizes and having supersaturation threshold of, say, 0.045% instead of 0.3%, sea-salt aerosols are preferentially activated when mixed with sulfate particles (O'Dowd et al., 1999). Activated sea-salt aerosols consume the available water vapor at low supersaturation thereby preventing the reach of the higher supersaturation needed for the activation of sulfate particles. Competition sets up between sea-salt and sulfate aerosols for water vapor. Increasing sea-salt aerosols with increasing wind reduces the number of activated sulfate aerosols under all conditions. The total number of activated CCN, however, either increases or decreases depending on the combination of sulfate concentration and updraft velocity (Ghan et al., 1998). Cloud albedo is most

susceptible to changes in CCN number in clean atmosphere (Murphy et al., 1998b). The addition of even some 10-20 CCN cm^{-3} into a clean marine air mass with some pre-existing 50 CCN cm^{-3} would have a considerable effect on cloud albedo (Andreae, 1995). Competition between sea-salt and SO_4^{2-} aerosols is important while the sea-salt particles are fresh and have a low supersaturation threshold. Aged sea-salt aerosols enriched with SO_4^{2-}, especially the accumulation mode ones, act as CCN just like all other SO_4^{2-} particles.

2.3.4 Atmospheric chemistry

Multiphase and heterogeneous reactions within sea-salt aerosols not only change their chemical composition, but also have far reaching consequences for other atmospheric constituents.

Reactive halogens

Sea-salt aerosols are the principle source of inorganic reactive halogens in the troposphere (Cicerone, 1981; Graedel and Keene, 1996; Keene et al., 1999). Dehalogenation of sea-salt aerosols releases gases containing Cl and Br, such as particulate Cl and Br, HCl and HBr, nitryl chloride ($ClNO_2$), molecular Cl_2 and Br_2, hypochlorous and hypobromous acids (HOCl, HOBr), BrCl (Pszenny et al., 1993; Graedel and Keene, 1995; Finlayson-Pitts and Pitts, 1997). Daytime photolysis of these chlorinated gases produces Cl and Br atoms, which act as oxidants in the troposphere. Halogen radicals oxidize organics, e.g., methane (CH_4) and dimethyl sulfide (DMS), 1-3 orders of magnitude faster than the conventional radicals such as hydroxyl radicals (OH) and ozone (O_3) (Keene et al., 1990; Finlayson-Pitts and Pitts, 1997). In polluted areas, where the liberation of Cl^- from sea-salt aerosols is enhanced,

Cl-atom oxidation of CH_4, a greenhouse gas, could be significant. In polar and remote ocean regions, where O_3 is in low concentrations, atomic Cl is the predominant oxidant (Finlayson-Pitts and Pitts, 1997).

Tropospheric ozone

In contrast to the man-made long-lived Cl-containing compounds, e.g., CFCs, which eventually reach the stratosphere and play a detrimental role for the ozone layer, most naturally halogenated species are quickly removed from the atmosphere by photolysis, oxidation, or dry and wet deposition (Graedel and Keene, 1995). Thus, they reside mostly in the troposphere and affect the concentration of surface ozone (O_3), which may cause two opposite effects. The positive side of the surface O_3 is that it is a source of OH, which is an active oxidant cleansing the atmosphere from most air pollutants (Crutzen and Zimmermann, 1991; Andreae and Crutzen, 1997; Finlayson-Pitts and Pitts, 1997). The negative side is that surface O_3 is an air pollutant itself with adverse impacts on human health (Finlayson-Pitts and Pitts, 1997) and is a greenhouse gas adding to global warming (IPCC, 2001). Photochemical reactions promoted by Cl and Br radicals enhance either the production or the destruction of surface O_3 (Keene et al., 1990). Cl/Br chemistry and scavenging of O_3 by sea-salt aerosols provide a net sink of surface O_3 in clean areas with low concentrations of nitrogen oxides (NO_x), which are necessary ingredients for O_3 formation (Keene et al., 1990). In polluted air with plenty of NO_x delivered from fossil fuel combustion, however, the same Cl/Br chemistry enhances the O_3 formation by supplying additional radicals, e.g., peroxy radicals (HO_2) from Cl-oxidation of hydrocarbons (Keene et al., 1990; Finlayson-Pitts and Pitts, 1997). Destruction of surface O_3 is still possible in polluted air if the NO_x are scavenged by numerous sea-salt aerosols and the Cl/Br

chemistry is more effective as an O_3 sink (Sander and Crutzen, 1996). The most dramatic destruction of surface O_3 is observed in polar regions due to Br chemistry, which is two orders of magnitude faster than Cl chemistry reactions (Barrie et al., 1988; Koop et al., 2000).

Sulfur cycle

Multiphase reactions within sea-salt aerosols couple them with the sulfur (S) atmospheric cycle (Chameides and Stelson, 1992; Luria and Sievering, 1991; Sievering et al., 1992; 1995). Worldwide outgasing of DMS from the oceans and subsequent oxidation by OH and NO_3 deliver sulfur dioxide (SO_2) to the marine atmosphere. Gas-phase and in-cloud oxidation of SO_2 by OH and H_2O_2 radicals, respectively, convert SO_2 to SO_4^{2-}. However, the formation of atmospheric SO_4^{2-} by these two processes alone does not balance with the SO_4^{2-} deposition. Chemical reactions within sea-salt aerosols provide an alternative way by mediating the formation and removal of about half of the measured SO_4^{2-} in the atmosphere. Sea-salt aerosols uptake gaseous SO_4^{2-} via H_2SO_4 scavenging. At pH 7, before sea-salt aerosols acidify, the aqueous-phase S is rapidly converted to nss SO_4^{2-} by O_3 oxidation within the aerosols. Coarse-mode sea-salt aerosols have a high deposition rate, from about 1 cm s^{-1} (Sievering et al., 1992) to 10-100 cm s^{-1}, and therefore quickly return 10 to nearly 100% of the S formed in the MBL from DMS back to the ocean. The combination of SO_4^{2-} conversion and removal by multiphase reactions within sea-salt aerosol in clear air and similar reactions in cloud drops formed on sea-salt CCN makes sea salt the largest sink for atmospheric S (Clegg and Toumi, 1998). The rapid exchange of S between the ocean and atmosphere would diminish the enhancement of

cloud albedo from the DMS precursor predicted by the Charlson et al. (1987) hypothesis.

In summary, the review in §§2.2 and 2.3 shows that ocean-produced sea-salt aerosols are the most numerous naturally emitted aerosols. In clean marine air, their physical, chemical, and optical properties control the baseline properties and climate effects of the total aerosol load. In the prospect of global warming, associated with higher winds, the emissions of sea-salt aerosols may increase and with that their role for climate (Latham and Smith, 1990; IPCC, 2001). Currently or in a future world with polluted air and a warmer climate, sea-salt aerosols have the potential to affect several climatic aspects: 1) Sea-salt aerosols can mitigate global warming directly by increasing planetary albedo, indirectly by adding CCN and altering cloud albedo, and chemically by removing CH_4 and surface O_3. 2) Sea-salt aerosols may diminish the cooling effect of sulfate aerosols by rapid removal of natural, formed out of DMS, and anthropogenic SO_4^{2-} from the atmosphere, and by preventing the activation of sulfate aerosols as CCN. 3) Sea-salt aerosols help maintain the oxidation capacity of the atmosphere, hence pollution cleaning, by enhancing the production of surface O_3 which sustains OH concentration. Therefore, the properties and effects of sea-salt aerosols must be adequately parameterized and included in climate models.

2.4 Generation function for sea-salt aerosols

2.4.1 Definition of the sea-salt generation function

Gong et al. (1997a) pioneered the inclusion of sea-salt aerosols as an active part of a climate model. To be realistic, a climate model has to simulate as many

processes affecting the sea-salt aerosol concentration and distribution as possible. Gong et al. (1997a) include in their model a comprehensive set of processes influencing sea-salt aerosols from their birth to their removal from the air, namely generation, transport, diffusion and convection, chemical and physical transformations in clear air, in clouds, and below clouds, and, finally, wet and dry deposition of sea-salt aerosols. The starting point to model the emission of sea-salt aerosols from the ocean surface is to model the generation of sea-spray droplets. The current study concentrates on the process of sea-salt aerosol generation.

A generation function of sea-spray droplets predicts how many film, jet, and spume drops are produced for each size of interest depending on the wind speed. Thus, the generation function of sea spray must include two major dependencies: dependence on droplet size at formation, r_0 in μm, and dependence on wind speed, usually measured at 10 m reference height, U_{10} in m s^{-1}:

$$\frac{dF(r_0, U_{10})}{dr_0} = f(U_{10}) \cdot f(r_0) \tag{2.1}$$

Some models parameterize sea-salt aerosols with size distributions (Winter and Chýlek, 1997; Jacobson, 2001a; Moldanová and Ljungström, 2001) at fixed wind speed, i.e., they rely on the size dependence only. If each production mechanism (film, jet, and spume drops) generates a lognormal distribution described with three parameters—mean radius, standard deviation, and total concentration—a tri-modal lognormal curve is constructed (O'Dowd et al., 1997) to represent sea-salt aerosols in the nucleation, accumulation and coarse modes. Reported measurements (Hoppel and Frick, 1990; O'Dowd and Smith, 1993; Quinn et al., 1996; Reid et al., 2001) provide values for the distribution parameters of each mode.

Other models predict how much sea-salt aerosols are generated in terms of total mass concentration (Erickson et al., 1986; Erickson and Duce, 1988; Tegen et al., 1997; Haywood et al., 1999), and rely on the wind dependence only. These models use an empirical expression in the form $C_m = e^{aU_{10}+b}$, C_m being the sea-salt mass concentration in μg m^{-3}, and a and b are regression coefficients, derived by fitting regression curves to measured sea-salt concentration under various winds (Lovett; 1978; Exton et al., 1985).

Indeed, different models pursue different purposes, and these parameterizations might be sufficient in some cases, yet the lack of one of the two required dependencies restricts investigations of possible additional results and interpretations. Gong et al. (1997a) used the generation function proposed by Monahan et al. (1986), which involves both wind and size dependencies.

2.4.2 Explicit form of the sea-salt generation function

The generation function of Monahan et al. (1986) is well respected for two reasons: i) it is the first generation function accounting for the indirect and direct production of sea-spray droplets; and ii) it models the bubble-mediated component of the sea spray well. A drawback of the generation function of Monahan et al. (1986) is that it overestimates the number of spume droplets (Burk, 1984; Stramska, 1987; Wu, 1993; Andreas, 1992, 1998). Gong et al. (1997a) encountered this problem and their model gave too many drops at high wind speeds.

Over the years, numerous field measurements gave a basis for refining this first attempt, and a host of variants for the explicit expressions of $f(U_{10})$ and $f(r_0)$ in (2.1) have been proposed (Andreas, 1992; 1998; Wu, 1993). Andreas (2002) reviewed 13 reported generation functions. To compare their performance, the author converted

them, when necessary, into (2.1) form, and unified them by size and measurement height. Andreas (2002) identified the spray generation function of Fairall et al. (1994) as currently the most reliable one. The specific form of this generation function is (Andreas, 2002):

$$\frac{dF}{dr_0} = 38W(U_{10})\, r_0^{-0.024}\, \frac{df}{dr_{80}} \qquad (2.2)$$

which gives the flux of spray drops produced per unit surface in a interval of drop sizes [m^{-2} s^{-1} μm^{-1}]. Here, $W(U_{10})$ is the whitecap coverage as a function of U_{10}:

$$W(U_{10}) = 3.8\times10^{-6} U_{10}^{3.41} \qquad (2.3),$$

r_{80} is the radius of a spray droplet at RH of 80%, and df/dr_{80} gives the size dependence with four different analytical parts covering radii r_{80} in the 0.8-250 μm range. Andreas (2002) recommends the Fairall et al. (1994) generation function because it spans the largest range of observed sea-spray droplets, has the theoretically predicted wind speed dependence, extends up to U_{10} values of 25 m s^{-1}, and gives appropriate number of sea-spray droplets.

Since (2.2) is the most general representation of the sea-salt generation function, any other required sea-salt aerosol variable (e.g., volume, surface, and mass flux, or number and mass concentration) could be derived from it.

The Fairall et al. (1994) generation function (2.2) must be used in climate models to evaluate sea-salt aerosol production because it is the most reliable generation function available for now and can be easily converted to any desired variable, which a climate model might need to describe the sea-salt aerosol emission and population.

2.4.3 Evaluation of the sea-salt generation function

The size dependence in the generation function (2.1) has been continuously refined by inclusion of field and laboratory measurements, as well as theoretical considerations (Andreas, 1998). This line of work has always been driven by the necessity to model correctly the spume droplets, which are important for the heat budget of the MBL (Andreas, 1992; Andreas et al., 1995). The size dependence in the generation function is well established and reliable in the size range from r_0 = 1.6 μm to 500 μm (Andreas, 2002).

The wind dependence in the generation function is introduced through whitecap coverage with the empirical expression (2.3) proposed by Monahan and O'Muircheartaigh (1980). This expression is well recognized in the sea spray community and widely used for estimating oceanic whitecaps (Erickson et al., 1986; Fairall et al., 1990; Frouin et al., 2001).

Thus, the required dependencies on U_{10} and r_0 in (2.2) are currently the best available.

Are any further improvements possible or are changes necessary for this generation function in order to meet the requirements of climate studies?

Regarding the size dependence, further improvement of the currently established $f(r_0)$ is desirable at the *large-size end* for better estimates of heat exchange. This could be achieved by incorporating new direct measurements of spume drops in the open ocean—a challenging endeavor under gale force winds (Andreas et al., 1995). Sea-salt aerosol sizes (in terms of radius at the formation, r_0) relevant for aerosol studies fall in the 0.1-20 μm range (§2.2.2, ***Size***). That is, from point of view of the climate studies, the current generation function is applicable only for the upper end of

the necessary size range of sea-salt aerosols. The current generation function, therefore, must be extended toward the *small-size end*.

Regarding the wind dependence, it has been shown that the variance of the measured sea-salt mass concentration with wind speed is high, from 0.16 to 0.88, i.e., local winds explain only 16% to at most 88% of the variance (Exton et al., 1985; Hoppel et al., 1989; Gong et al., 1997a; Quinn and Coffman, 1999; Reid et al., 2001). This implies that in addition to particle size and wind, the production of sea-salt aerosols is affected by other factors not accounted for in the generation function (2.2).

Other environmental parameters can be introduced in (2.2) via whitecap coverage. Any variable that influences the surface wind field, the frequency of wave breaking, and the processes of bubble formation and bursting influences whitecap coverage as well. This, in turn, affects the production of sea-spray droplets, and ultimately the generation of sea-salt aerosols. Expanding the wind dependence $W(U_{10})$ in the generation function (2.2) to include additional factors may render a more realistic modeling of sea-salt aerosol emission.

These considerations set one of the major goals of the current study, and introduce whitecaps as another subject of investigation besides sea-salt aerosols.

2.5 Oceanic whitecaps

The wind blows, waves form and break, bubbles form and burst, spray drops form and evaporate, finally sea-salt aerosols form—we witness this sequence of processes whenever we see whitecaps in the ocean. The whitecaps are comprised of bubble clouds beneath and foamy patches on the water surface. Both these parts are mixtures of water and air in different quantities representing different types of foam (Adamson, 1982; Weaire and Hutzler, 1999). Bubble bursting and sea-salt aerosol

formation take place within the superficial foam of the whitecaps. Whitecap coverage, W, denotes the fraction of the ocean surface covered by these foamy patches.

Blanchard (1963) estimates average whitecap coverage of 3-4% of the ocean surface. This small fraction of ocean surface generates 90% of the total amount of sea-salt aerosols. A background bubble population exists, which produces sea spray over 100% of the sea surface, but its contribution to the total sea-salt aerosol production is only 10%. Whitecap coverage, therefore, is a true representation of the ocean area actively producing sea-salt aerosols.

2.5.1 Factors affecting the whitecap coverage

Whitecaps start to appear at wind speeds above 3 m s^{-1} (Monahan and O'Muircheartaigh, 1986). Wind speed is the most influential among all possible variables. A power law in the form $W = aU_{10}^{\ b}$ with an analytically predicted value of b of about 3 is accepted to describe the dependence of whitecap coverage on wind speed (Blanchard, 1963; Monahan and O'Muircheartaigh, 1986; Wu, 1979, 1992b). The specific values of a and b in (2.3) are obtained with statistical analysis and are the optimal ones (Monahan and O'Muircheartaigh, 1980). Currently, $W(U_{10})$ is the only relation well understood and quantified.

Monahan and O'Muircheartaigh (1986) suggest that atmospheric stability (the difference between seawater and air temperatures), ΔT, water temperature, T_s, water salinity, S, wind fetch, f, wind duration, d, and surfactant concentration, C, may influence oceanic whitecap coverage as well. Among these, only the $W(\Delta T)$ relation is quantified:

$$W = 1.95 \times 10^{-5} U_{10}^{2.55} \exp(0.086 \Delta T) \qquad (2.4)$$

If ΔT, defined as the difference between the water and air temperatures, changes from +1 to -1 ^{o}C at constant U_{10}, the W decreases by more than 15%.

The dependence of W on the remaining factors (T_s, S, f, d, and C) is only qualitatively discussed (Monahan and O'Muircheartaigh, 1986; Reid et al., 2001). With T_s increasing, the exponent b, hence W, increases for two reasons: water viscosity, n, decreases and the lifetime, t_W, of an individual whitecap increases with rising T_s. Longer d in open regions produces a fully developed sea, which increases b and W. In contrast, d is small in constrained places and even high winds would produce fewer whitecaps, thus b and W decrease. An increase in T_s additionally boosts the effect of long d since usually open regions have warm waters, e.g., trade wind regions. The opposite is also true—most restricted areas have cold waters, e.g, Gulf of Alaska. One important exception is the Southern Ocean where the effect of long d is probably suppressed by the opposite effect of low T_s. Fewer whitecaps form in places with limited f. The effect of f and its relation to T_s are analogous to those of d and T_s. Whitecaps in seawater are more persistent compared to those in fresh water (Monahan and Zietlow, 1969; Scott, 1975). Small variations of S in the open ocean would most probably not cause noticeable variations in W, but S differences in the open ocean and coastal zones could invoke measurable changes in W. Finally, organic compounds create surface-active film on the open ocean surface and slow down, or even prevent, the breaking process yielding a decrease in W (Scott, 1986). In contrast, surfactants on the bubble walls stabilize the bubbles and inhibit their coalescence (Blanchard, 1983; Scott, 1986), which prolongs t_W and W increases.

Overall, while additional factors affecting W are identified and qualitatively understood, quantifications of any of the relations $W(T_s, S, f, d, C)$ are missing. To

extract empirical expressions for each of these additional dependences, a database of whitecap coverage under various environmental and meteorological conditions is necessary. Do existing measurements of whitecap coverage provide enough data to compile such a database?

2.5.2 Whitecap coverage measurements

Data sets of whitecap coverage have been collected from research platforms, ships, and aircraft. W is derived from photographs of the sea surface, the analysis of which is somewhat subjective and adds uncertainty to W values (Blanchard, 1963; Monahan, 1971; Nordberg et al., 1971; Stogryn, 1972; Ross and Cardone, 1974; Bondur and Sharkov, 1982). Table 2.1 summarizes facts for 16 data sets reported in the literature. Figure 2.2 shows the locations of measurements, and demonstrates well the patchiness of the conditions represented. Experiments held for a time span of 30 years provide about 500 data points! The conditions encountered cover: i) a wind speed range of 0.1-25 m s^{-1}, Figure 2.3a; ii) a range of ΔT conditions from –8 to +7 ^{o}C (Monahan and O'Muircheartaigh, 1986); and, iii) water temperatures from -1.7 to 30.55 ^{o}C, Figure 2.3b. While the wind speed and stability conditions are well represented and ensure an empirical derivation of $W(U_{10})$ and $W(\Delta T)$, eq. (2.3) and (2.4), the T_s range is represented in discrete intervals and cannot be used confidently to extract $W(T_s)$. Only two of these datasets report values for f (Monahan, 1971; Ross and Cardone, 1974). The remaining parameters (S, d, and C)

Table 2.1 Data sets of whitecap coverage observations

No	Dataset	Data points	Relative error %	Location	Time	Method	U_{10} range [m s^{-1}]	T_s [^{o}C]	Add. param. ΔT, S, f, d, C	Reference
1	US Squadron	5	NA	Caribbean area	Jun-Oct, 1952	Aerial photos	4–20.6	NA	NA	Blanchard, 1963
2	Nea	4	15	North Sea North Atlantic	Mar, 1969	Aerial photos	13–25	2–9 Tabulated	ΔT tabulated	Nordberg et al., 1971
3	BOMEX	38	7–91	Barbados, Atlantic Ocean	May, 1969	Photos	2.9–9	28–28.65 Tabulated	f tabulated ΔT tabulated	Monahan, 1971
4	M71	16	7–100	West Atlantic Coast	Jul-Aug 1969	Photos	0.1–17.7	17.4–30.55 Tabulated	f tabulated ΔT tabulated	Monahan, 1971
5	RC	13	21–168	North Sea, Atlantic Caribbean Sea	Mar, 1969 Jan, 1971	Aerial photos	9.7–23.3	NA	f tabulated ΔT tabulated	Ross and Cardone, 1974
6	TC	29	NA	East China Sea	1972?	Photos	8.5–18.8	24.7 Mean value	NA	Toba and Chaen, 1973
7	Kea	6	NA	Observation Tower Hiratsuka, Japan	1972?	Photos	5–14	14.8– 6 Range	NA	Kondo et al., 1973
8	MMM	6	NA	NA	1975, 1978	Aerial photos	15–25	NA	NA	Bortkovskii, 1987
9	Typhoon-75 Typhoon-78	39	22	Western Tropical Pacific	1975, 1978	Photos	5–15	27–29 Range	f, C qualitatively	Bortkovskii, 1987 (1 in Fig. 2.5)
10	JASIN	64	13–396	NE Atlantic	Aug-Sep 1978	Photos	2.5–15.3	12.5–14 Tabulated	ΔT tabulated	Monahan et al., 1983b
11	STREX	84	13–200	Gulf of Alaska	Nov-Dec, 1980	Photos	2.7–17.2	5.11–11.11 Tabulated	ΔT tabulated	Doyle, 1984
12	RV-Bugaev	34	40	North Atlantic Kuroshio	1979-1980 1983	Photos	9–24	3–15 10–23 Ranges	f, C qualitatively	Bortkovskii, 1987 (2 in Fig. 2.5)
13	BS	3	80–126	Black and Barents seas	1981?	Aerial photos	5.7–10.5	≤ 12 Mean value	NA	Bondur and Sharkov, 1982
14	POLEX-YUG	31	40	Seas Scotia, Weddell, Bellingsgausen	Dec 1981 Mar 1982	Photos	8.5–18	-1.7 +3 Range	f, C qualitatively	Bortkovskii, 1987 (3 in Fig. 2.5)
15	MIZEX83	32	6–200	NorthAtlantic Arctic Ocean	Jun-Jul 1983	Photos	4.7–14	-1.3–14.4 Tabulated	ΔT tabulated	Monahan et al., 1984
16	MIZEX84	102	14–650	NorthAtlantic Arctic Ocean	Jun-Jul 1984	Photos	2.6–16.4	-1.17–9.9 Tabulated	ΔT tabulated	Monahan et al., 1985

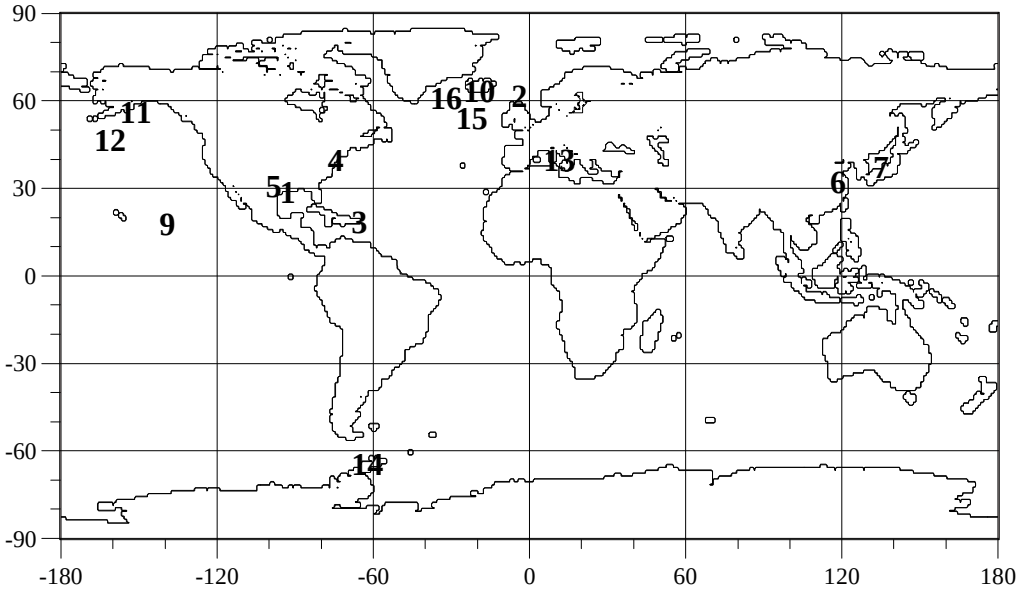

Figure 2.2 Locations of the whitecap measurements summarized in Table 2.1 (Location numbers correspond to the list number of the experiments in the Table).

are not reported. Spatially and timely averaged values for *S*, *d*, and *C* could be inferred from the experiment locations, but these order of magnitude estimations would not reflect the true conditions which had accompanied the measurements of *W*. Therefore, the existing measurements of whitecap coverage are not enough to organize an adequate database of *W* with concomitant values of environmental and meteorological conditions. An alternative approach, ensuring a complete representation of *W* and the additional factors, is to derive values of the whitecap coverage on a global scale. To

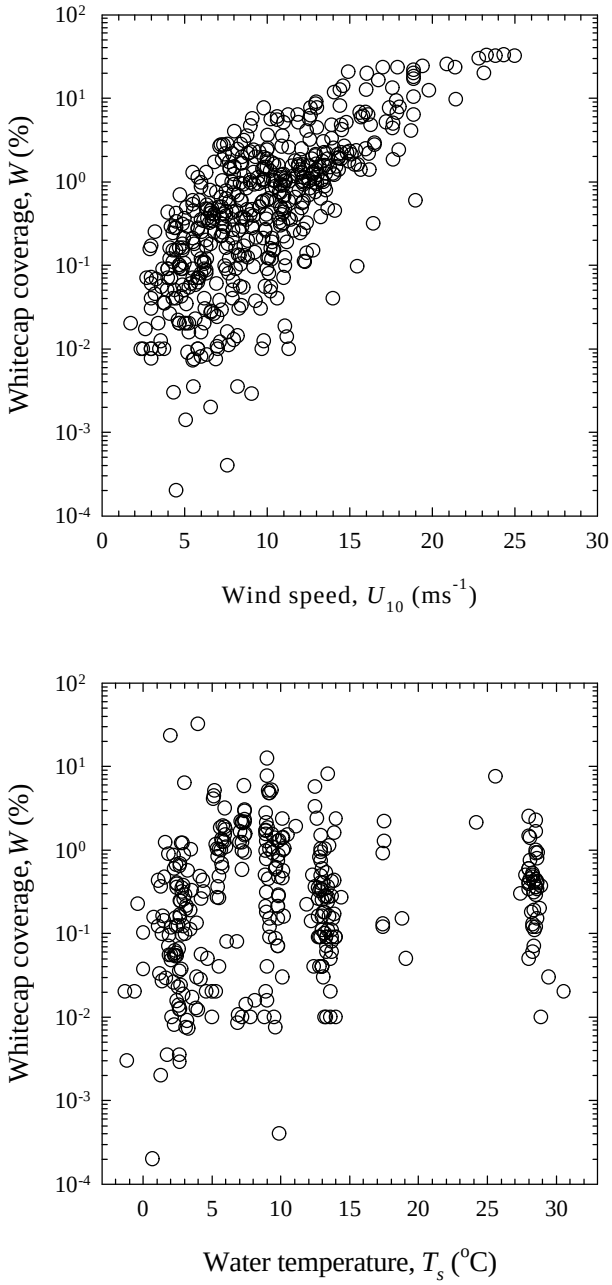

Figure 2.3 ***In situ*** **measurement of whitecap coverage, *W*, as a function of: a) wind speed, U_{10}; b) water temperature, T_s.**

achieve this goal, it is necessary to find a relation of W to a variable, which can be obtained from current satellite measurements.

2.5.3 Remote sensing signatures of whitecaps

Wavelength-dependent changes of whitecap reflectivity, r_f, and emissivity, e_f, make them detectable by remote sensors in different portions of the electromagnetic spectrum (ems) (Koepke, 1986; Monahan and O'Muircheartaigh, 1986).

In the visible and near-infrared portions of the ems, foam reflectivity is about 10 times higher than that of the surrounding water ($r_f \approx 22\%$ compared to 2% of seawater), and is the reason we spot and photograph whitecaps on the ocean surface as bright white patches. According to Kirchoff's law, reflection, r, absorption, a, and transmission, t, in any medium add to unity, and since in the ocean $t \cong 0$, $r + a = 1$ (Maul, 1985; Stewart, 1985; Swift, 1990). The conservation of energy law requires whatever energy is absorbed to be emitted, i.e., $a = e$. Therefore, the high reflectivity of the whitecaps in the visible is necessarily complemented with little absorption, hence little emission. By contrast, in the microwave region, whitecaps are poor reflectors, but excellent emitters with emissivity, e, close to 1. The switch between these two extrema is in the infrared portion of the ems, where whitecap reflectivity gradually decreases while the emissivity gradually increases providing measurable yet small signals for detection.

Due to these whitecap signatures, remote sensors can detect changes in the radiation reflected or emitted by foam-covered ocean surface compared to that reflected or emitted by foam-free ocean. Whitecap-induced changes in ocean reflection and emission are sufficiently large to allow registering signals from a foam-covered

ocean with a high signal-to-noise ratio. How do different satellite-borne sensors at the top of the atmosphere capture such changes?

2.5.4 Whitecap detection from satellites

A remote sensor working at visible wavelengths registers ocean radiance. Currently Sea-viewing Wide-Field-of-view Sensor (SeaWiFS) (Hooker et al., 1992) and Moderate Resolution Imaging Spectroradiometer (MODIS) (Esaias et al., 1998) measure radiation reflected by the ocean surface at the top of the atmosphere, and via calibration with the sun's incident radiation obtain r directly. A remote microwave sensor registers surface emission as brightness temperature, T_B, which relates to the physical surface temperature, T_s, through e:

$$T_B = eT_s \tag{2.5}$$

According to (2.5), at certain T_s of the seawater and foam, whitecaps would have elevated T_B compared to that of ocean surface free of whitecaps due to their higher e. Thus, while bright white spots in the visible, whitecaps are like "hot" spots on the cold ocean surface in the microwave part of ems. Williams (1969) first recognized the significance of relation (2.5) for microwave remote sensing techniques. The Special Sensor Microwave Imager (SSM/I) detects the naturally emitted radiation from the ocean surface as T_B (Hollinger, 1990).

Therefore, the remotely sensed variables suitable for retrieving whitecap coverage from satellite measurements are reflection, r, in the visible and brightness temperature, T_B, in the microwave regions.

SSM/I-measured T_B is the preferred choice for deriving W on the ocean surface because the atmospheric intervention on a signal detected in the microwave region is less than that in the visible (Stewart, 1985; Swift, 1990). In both regions of

the ems, clouds, rain, and atmospheric gases all add to the radiation carrying useful information for ocean surface phenomena by scattering and emission. In the visible, the signal from the intervening atmosphere is about 90% of the total signal detected at the top of the atmosphere (Gordon and Wang, 1994), while at 5 GHz it is a 4% problem (Swift, 1990). The procedure of removing the undesired atmospheric signal is termed as the atmospheric correction. The ocean color algorithm, for instance, which derives information for the primary productivity in the ocean from SeaWiFS and MODIS data, has an elaborate scheme of atmospheric correction (Gordon and Wang, 1994). The necessity for atmospheric correction in the microwave range exists, but is not as severe as for the visible range, because clouds are almost transparent to the long wavelengths and fewer atmospheric constituents influence the signal from the ocean surface.

The avoidance of the atmospheric attenuation problem at microwave frequencies is at the expense of losing resolution. An instrument working in the microwave range of the ems requires a larger antenna than an instrument working at visible frequencies (Stewart, 1985; Swift, 1990). None of the current satellite-borne microwave sensors, even with the least antenna footprint of 9 km $\times$ 9 km, can resolve an individual whitecap having a length scale of at most 10 m (Bortkovskii, 1983; Dahl and Jessup, 1995). Whitecap coverage detection, however, does not necessitate resolving and counting individual whitecaps. Rather, it is of interest how much the *average* emission of a given ocean surface area changes if 1%, 10% or more of this area is covered with whitecaps and how well these changes can be retrieved from measured T_B values.

Thus, the emissivity of oceanic whitecaps, e, is reliably connected to the brightness temperature, T_B, measured daily by SSM/I, and this relation can be used to

estimate whitecap coverage, W, globally. Devising a method for retrieving W from T_B emerges as the other major goal of this study.

2.6 Scientific objectives

The importance of sea-salt aerosols, produced within oceanic whitecaps, for the radiative forcing of the climate system motivates this research. The review in the preceding sections justifies three basic topics and helps formulate the specific goals of the current study:

1) Global whitecap coverage:
   - Develop a new method for estimating whitecap coverage on a global scale using the microwave emissivity of the ocean surface.

2) Whitecap coverage database:
   - Build a representative database of whitecap coverage estimates concomitant with environmental variables using the new method.
   - Examine spatial and temporal characteristics of global whitecap coverage.
   - Evaluate the contribution of whitecaps to various air-sea and climatic processes.
   - Parameterize the dependence of whitecap coverage on water temperature and salinity using the whitecap coverage database.

3) Generation of sea-salt aerosols:
   - Modify the existing generation function of sea-salt aerosols by:
     - Including whitecap coverage containing the effects of additional factors;
     - Extending it to smaller sizes.
   - Estimate sea-salt aerosol loading using the modified generation function.
   - Investigate spatial and temporal characteristics of sea-salt aerosols.

- Investigate the performance of the modified generation function.
- Evaluate the contribution of sea-salt aerosols to various climatic processes.